Targeting hyperactive platelet-derived growth factor receptor-β signaling in T-cell acute lymphoblastic leukemia and lymphoma

Stien De Coninck,[1,2] Renate De Smedt,[1,2] Béatrice Lintermans,[1,2] Lindy Reunes,[1,2,3] Hansen J. Kosasih,[4,5] Alexandra Reekmans,[1,2] Lauren M. Brown,[4,5] Nadine Van Roy,[2,6,7] Bruno Palhais,[1,2,3] Juliette Roels,[1,2] Malaika Van der Linden,[2,8] Jo Van Dorpe,[2,8] Panagiotis Ntziachristos,[2,3] Frederik W. van Delft,[9] Marc R. Mansour,[10] Tim Pieters,[2,3] Tim Lammens,[2,11,12] Barbara De Moerloose,[2,12] Charles E. de Bock,[4,5#] Steven Goossens[2,13#] and Pieter Van Vlierberghe[1,2#]

[1]Lab of Normal and Malignant Hematopoiesis, Department of Biomolecular Medicine, Ghent University, Ghent, Belgium; [2]Cancer Research Institute Ghent (CRIG), Ghent, Belgium; [3]Department of Biomolecular Medicine, Ghent University, Ghent, Belgium; [4]Children's Cancer Institute, Lowy Cancer Research Centre, UNSW Sydney, Kensington, New South Wales, Australia; [5]School of Clinical Medicine, UNSW Medicine and Health, UNSW Sydney, Sydney, New South Wales, Australia; [6]Lab for Translational Oncogenomics and Bioinformatics, Department of Biomolecular Medicine, Ghent University, Ghent, Belgium; [7]Pediatric Precision Oncology Lab, Department of Biomolecular Medicine, Ghent University, Ghent, Belgium; [8]Department of Pathology, Ghent University and Ghent University Hospital, Ghent, Belgium; [9]Wolfson Childhood Cancer Research Centre, Newcastle University Centre for Cancer, Newcastle upon Tyne, UK; [10]Department of Developmental Biology and Cancer, Institute of Child Health, University College London, London, UK; [11]Department of Internal Medicine and Pediatrics, Ghent University, Ghent, Belgium; [12]Department of Pediatric Hematology-Oncology and Stem Cell Transplantation, Ghent University Hospital, Ghent, Belgium and [13]Unit for Translational Research in Oncology, Department of Diagnostic Sciences, Ghent University, Ghent, Belgium

[#]CEdB, SG and PVV contributed equally as senior authors.

Correspondence: S. Goossens
steven.goossens@ugent.be

Received: August 17, 2023.
Accepted: November 2, 2023.
Early view: November 9, 2023.

https://doi.org/10.3324/haematol.2023.283981

Abstract

T-cell acute lymphoblastic leukemia (T-ALL) and T-cell lymphoblastic lymphoma (T-LBL) are rare aggressive hematologic malignancies. Current treatment consists of intensive chemotherapy leading to 80% overall survival but is associated with severe toxic side effects. Furthermore, 10-20% of patients still die from relapsed or refractory disease providing a strong rationale for more specific, targeted therapeutic strategies with less toxicities. Here, we report a novel *MYH9::PDGFRB* fusion in a T-LBL patient, and demonstrate that this fusion product is constitutively active and sufficient to drive oncogenic transformation *in vitro* and *in vivo*. Expanding our analysis more broadly across T-ALL, we found a T-ALL cell line and multiple patient-derived xenograft models with PDGFRB hyperactivation in the absence of a fusion, with high PDGFRB expression in TLX3 and HOXA T-ALL molecular subtypes. To target this PDGFRB hyperactivation, we evaluated the therapeutic effects of a selective PDGFRB inhibitor, CP-673451, both *in vitro* and *in vivo* and demonstrated sensitivity if the receptor is hyperactivated. Altogether, our work reveals that hyperactivation of PDGFRB is an oncogenic driver in T-ALL/T-LBL, and that screening T-ALL/T-LBL patients for phosphorylated PDGFRB levels can serve as a biomarker for PDGFRB inhibition as a novel targeted therapeutic strategy in their treatment regimen.

Introduction

T-cell acute lymphoblastic leukemia (T-ALL) and T-cell lymphoblastic lymphoma (T-LBL) are aggressive subtypes of leukemia affecting the T-cell lineage. Since T-ALL and T-LBL patients have similar immunophenotypic, morphological and molecular genetic features, they are considered the same disease according to the World Health Organiza-

tion.[1] They are distinguished based on the infiltration into the bone marrow (BM); T-LBL cases have less than 25%, while T-ALL cases have more than 25% lymphoblasts in their diagnostic BM.[2] Patients can be classified into different molecular genetic subtypes based on the aberrant expression of specific oncogenic transcription factors, such as *LYL1*, *TLX1*, *TLX3*, *HOXA*, *NKX2-1*, *TAL1* or *LMO2*.[3,4] Current T-ALL/T-LBL treatment protocols consist of intensive chemotherapy followed by hematopoietic stem cell transplantation (HSCT) in high-risk or relapsed cases.[2,5] Treatment intensification resulted in improved overall survival (OS) rates for pediatric patients, nowadays reaching 80%.[6] However, OS rates remain low for adult patients (only 40%) with limited salvage options for refractory disease.[2,7] In addition, due to associated short- and long-term toxic side effects, the limit of tolerability for this intensified chemotherapy has been reached. Therefore, to improve the outcomes of patients with T-ALL/T-LBL, new targets for the development of more effective therapeutic strategies with less adverse side effects must be identified.

Protein kinase inhibitors are currently being investigated as targeted therapy for T-ALL/T-LBL, specifically in cases harboring activating kinase mutations.[8] Activating mutations in the IL7R-JAK-STAT pathway are present in 20-30% of T-ALL cases[9] and found to be sensitive to the Janus kinase (JAK) inhibitor ruxolitinib.[10] The *NUP214::ABL1* fusion is the most common ABL1 aberration in T-ALL and sensitive to the broad spectrum kinase inhibitor dasatinib.[11] Interestingly, high expression of the lymphocytic-specific kinase LCK is also found in T-ALL/T-LBL and can be used as a biomarker of dasatinib sensitivity.[12-14]

Platelet-derived growth factor receptor B (PDGFRB) is a member of the class III tyrosine kinase receptors. The extracellular part of the receptor has 5 immunoglobulin-like domains that can bind PDGF, the receptor ligands. In the absence of ligand, the receptor is inactive.[15] Upon ligand binding, PDGFR monomers dimerize, bringing the cytoplasmic tyrosine kinase domains into proximity, resulting in autophosphorylation of the receptor dimer. The phosphorylated receptor-receptor-complex is internalized and downstream signaling of PI3K/AKT, RAS/MAPK and JAK/STAT is activated, promoting cellular proliferation, differentiation, survival and migration.[16] Multiple translocations involving the PDGFRB locus have been reported in T-ALL/T-LBL including *ETV6::PDGFRB*,[17] *DOCK2::PDGFRB*,[18] and *AGGF1::PDGFRB*.[19] These fusions are all characterized by the 3' PDGFRB kinase domain placed under the control of their 5' fusion partner which favors dimerization resulting in ligand-independent constitutive activation.[15,20]

In this study, we report a novel *MYH9::PDGFRB* fusion in a pediatric T-LBL patient. We demonstrate that enforced expression is sufficient to transform cells to cytokine-independent growth *in vitro* and drive leukemia *in vivo*. Our study also implicates ectopic activation of PDGFRB as a more general oncogenic event in the absence of a chromosomal translocation in T-ALL/T-LBL and investigated the therapeutic potential of targeting this hyperactive PDGFRB in T-LBL/T-ALL using a selective PDGFRB inhibitor, CP-673451.

Methods

Detection and amplification of *MYH9::PDGFRB* fusion

The *MYH9::PDGFRB* fusion transcript was identified by Targeted Locus Amplification according to a previously described protocol.[21] Details and complete coding sequence of identified fusion product can be found in the *Online Supplementary Appendix*.

Expression plasmid and retrovirus production

The full length *MYH9::PDGFRB* fusion transcript was cloned into a pMIGII-IRES-GFP (MSCV) expression plasmid. Retrovirus production using HEK293T cells and transduction of Ba/F3 cells was performed as previously described.[22] Details are provided in the *Online Supplementary Appendix*.

Syngeneic bone marrow transplant

Lineage negative cells were isolated from the BM of 6-8 week old C57BL/6JAusB mice (Australian Bioresources, Australia) using the EasySep™ Mouse Hematopoietic Progenitor Cell Isolation Kit (#19856, Stemcell™ Technologies) according to the manufacturer's instructions. Retroviral vectors encoding the MSCV-MYH9::PDGFRB-IRES-GFP were transduced into hematopoietic stem and progenitor cells (HSPC) and then 1 million transduced cells were injected into the tail veins of sublethally irradiated (6 Gy) C57BL/6JAusB female recipients. Blood samples were taken at regular time points and analyzed on a BC5000 Hematology Analyzer (Mindray) and flow cytometry (MACSQuant® VYB, Miltenyi Biotec) to determine the evolution in white blood cells (WBC) and GFP^+ cell counts, respectively. Mice were sacrificed when the WBC counts exceeded $600x10^9$/L and/or ethical end point criteria were reached. Animal experiments were approved by the UNSW animal care and ethics committee (ACEC number: 23/11B).

Cell lines and patient samples

Cell lines (CTV-1, SEM, Jurkat, MOLT-16, DND-41, HEK293T) were purchased from the DSMZ repository (Braunschweig, Germany) and cultured in RPMI 1640 medium supplemented with 10% fetal bovine serum (FBS) at 37°C with 5% CO_2. Ba/F3 cells were maintained in 10% RPMI and 10 ng/mL recombinant murine interleukin-3 (PeptroTech). Primary T-ALL cells for *in vitro* and *in vivo* CP-673451 treatment were acquired by informed consent from the Department of Pediatric Hematology-Oncology at Ghent University Hospital. T-ALL patient-derived xenograft (PDX) samples were obtained from the laboratory of Prof. Richard B. Lock as described,[23] with details found on PedcBioPortal (PedcBio-

Portal KidsFirst (kidsfirstdrc.org)) depository.[24] Whole exome sequencing data of these PDX models is publicly available on PedcBioPortal in the PPTC, Maris, 2019 database and annotated as ETP1=T-ALL6; ETP3=T-ALL7; ETP6=T-ALL9.

Cell viability assays

Viable cells were counted using MACSQuant VYB Flow Cytometer (Miltenyi Biotec). Alternatively, CellTiter-Glo (Promega) assay was performed at indicated time points followed by measurement of luminescence using Glomax Discover Microplate Reader (Promega). Ratios of either cell numbers or signal from metabolically active cells in CP-673451 to DMSO were plotted to calculate IC_{50} values.

In vivo treatment of T-ALL patient-derived xenograft model with CP-673451

NSG-SGM3 (#013062, The Jackson Laboratory) 10-week old female mice (N=12) were intravenously injected with $2x10^6$ PDX cells. At regular timepoints, % hCD45 (130-114-569, Miltenyi Biotec) was measured using flow cytometry (BD LSR II Flow Cytometer) in peripheral blood (PB). After evidence of leukemic cell engraftment, mice were randomly divided into vehicle treatment (90% PEG300, 10% N-methylpyrrolidone) (N=5) and CP-673451-treatment (Bio-Connect) (N=7). CP-673451 was administered daily via intraperitoneal injection at a dose of 20 mg/kg (5 days on / 2 days off; total of 10 administration doses). During the experiment, leukemic burden was evaluated via %hCD45 in PB. Experiments were performed according to the ethical guidelines under UGent regulations, with approval of the ethical committee for laboratory animal experimentation of the Faculty of Medicine and Health Sciences.

Statistical analysis

Statistical power was calculated before every experiment (80% statistical power, α=0.05). The Shapiro-Wilk test was used to check for normality of data. Results are expressed as mean ± standard deviation where appropriate. Kaplan-Meier curves were used for the survival of mouse BM tranplants (BMT). For the comparison of 2 groups, an unpaired *t* test with Welch's correction or Mann-Whitney test was used. GraphPad Prism 9 (GraphPad Software Inc., La Jolla, CA, USA) was used to analyze the data.

For detailed methodology, see the *Online Supplementary Methods*.

Results

A novel *MYH9::PDGFRB* fusion gene identified in a T-cell lymphoblastic lymphoma patient can transform Ba/F3 cells to cytokine-independent growth

A 7-year old boy was diagnosed with T-LBL with 12% lymphoblasts found in the BM. (Additional clinical details are provided in the *Online Supplementary Appendix*). Array Comparative Genomic Hybridization (aCGH) was performed on a diagnostic sample and revealed a series of chromosomal imbalances, including gains and deletions (*Online Supplementary Figure S1A*). A chromosomal aberration was detected with potential partial loss of the 5q32 region, involving the *PDGFRB* locus. Using *PDGFRB* as a viewpoint, targeted locus amplification in combination with next generation sequencing identified a fusion between *MYH9* (Chr22) and *PDGFRB* (Chr5), in which the extracellular domain of PDGFRB is replaced by the motor domain of MYH9 which is a member of the P-loop NTPase fold family (Figure 1A, *Online Supplementary Figure S1B*).[25] Compared to healthy samples, increased PDGFRB protein levels were detected in both diagnostic and relapse samples of this T-LBL patient, using immunohistochemistry with a specific anti-PDGFRB antibody detecting the carboxyterminal fragment of the protein (Figure 1B). Unfortunately, no live cells were available from this patient.

We next sought to evaluate the oncogenic potential of the identified *MYH9::PDGFRB* fusion gene using IL-3 dependent mouse pro-B Ba/F3 cells. The full length *MYH9::PDGFRB* cDNA was amplified and cloned into the retroviral MSCV-IRES-GFP expression plasmid and then used to stably transduce Ba/F3 cells. In the absence of IL-3, expression of MYH9::PDGFRB was sufficient to drive cytokine-independent proliferation (Figure 1C). Expression of MYH9::PDGFRB was confirmed at the protein level as well as the constitutive activation of PDGFRB as reflected by high levels of phosphorylation of PDGFRB (Y751) (*Online Supplementary Figure S2A*). CP-673451 is a commercially available selective PDGFRB inhibitor, which can prevent phosphorylation of the wild-type PDGFRB receptor in the presence of PDGF-BB ligand activation (*Online Supplementary Figure S2B*). We tested whether CP-673451 could also inhibit hyperactivation of the MYH9::PDGFRB fusion. Ba/F3 cells transduced with MYH9::PDGFRB were highly sensitive to CP-673451 (IC_{50}=9.448 nM) compared to the activating JAK3(M511I) mutant control (no PDGFRB, *Online Supplementary Figure S2A*) that was resistant to CP-673451 (Figure 1D). Treatment also resulted in complete loss of PDGFRB (Y751) phosphorylation (pPDGFRB) and concomitant decrease in downstream STAT5 (Y694) phosphorylation (Figure 1E, F).

MYH9::PDGFRB drives acute leukemia in a murine bone marrow transplant model

Having established that MYH9::PDGFRB can transform pro-B Ba/F3 cells to cytokine-independent growth *in vitro*, we next used a syngeneic BM transplant model to determine whether the fusion product was also able to transform HSPC *in vivo* (Figure 2A). HSPC isolated from C57BL/6JAusB donor mice were retrovirally transduced with a vector expressing the *MYH9::PDGFRB* fusion or the *EBF1::PDGFRB* fusion, a well-described fusion gene in Philadelphia-like B-cell acute lymphoblastic leukemia.[26] Transduced cells were injected into sublethally irradiated female C57BL/6JAusB mice and

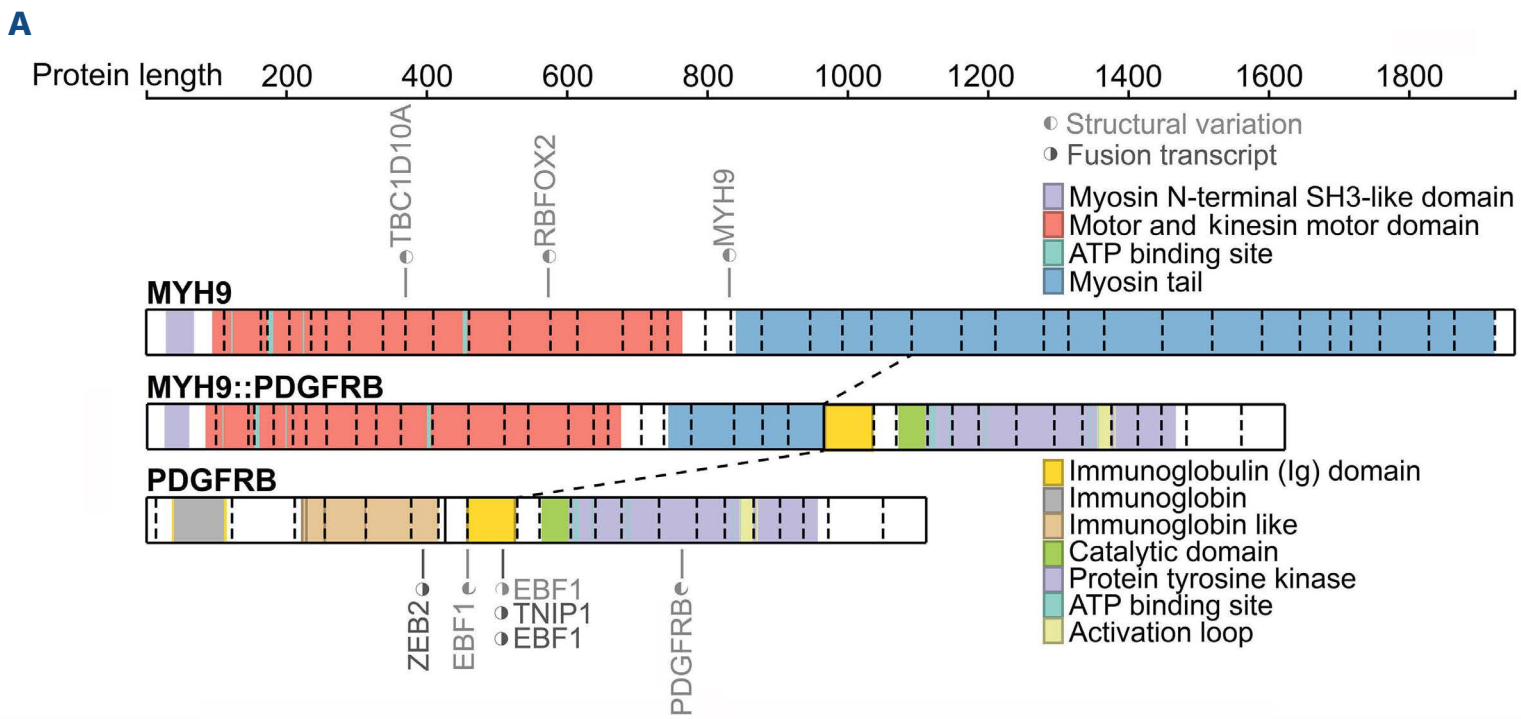

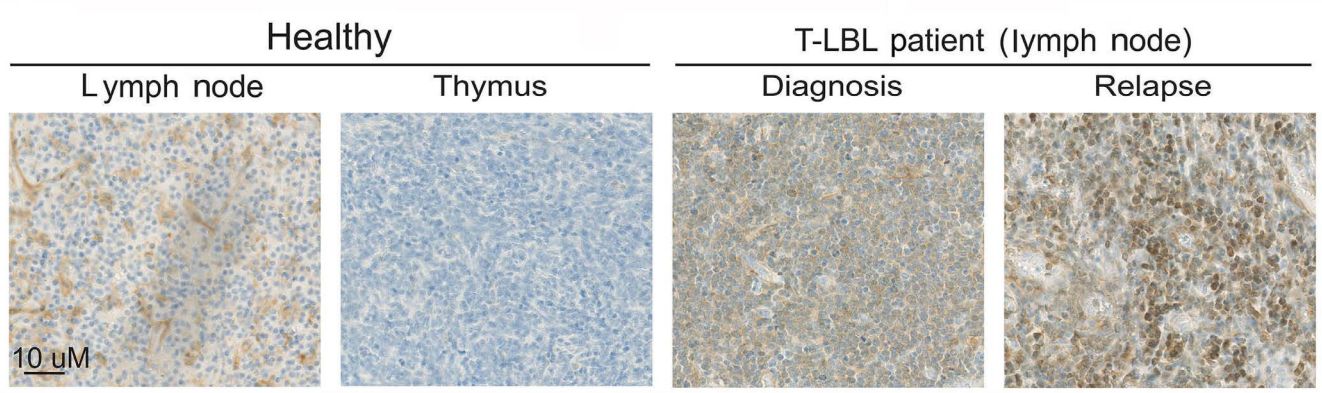

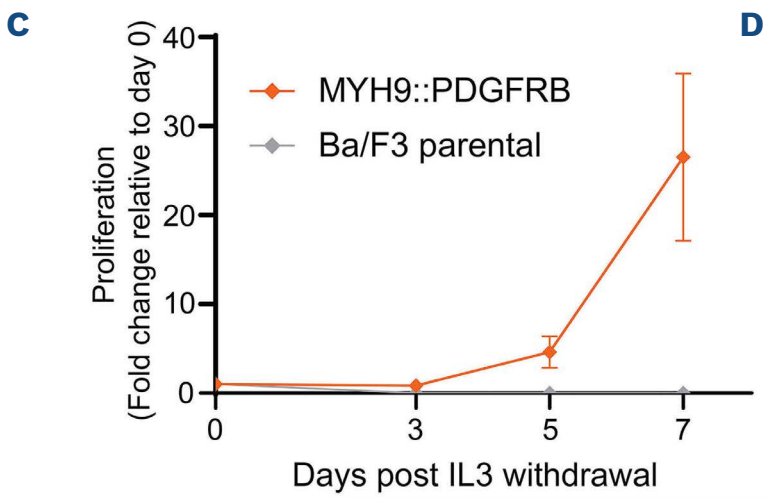

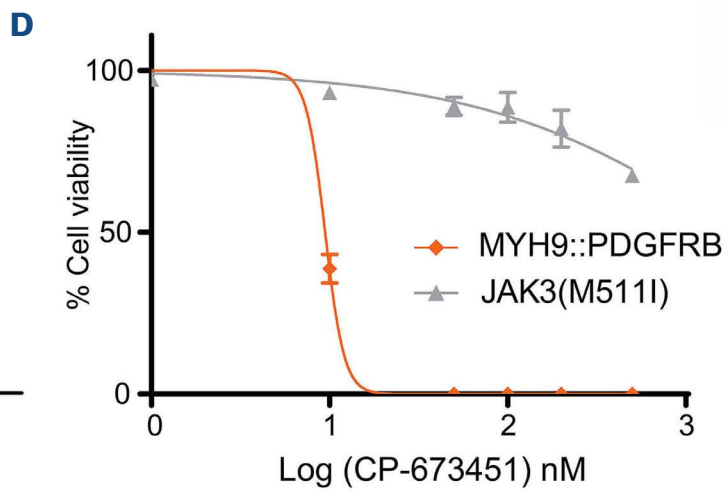

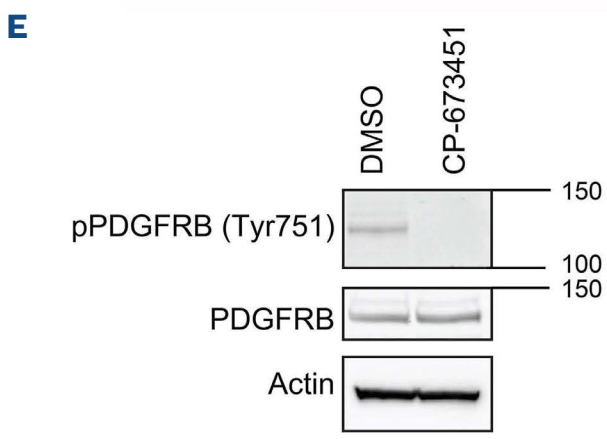

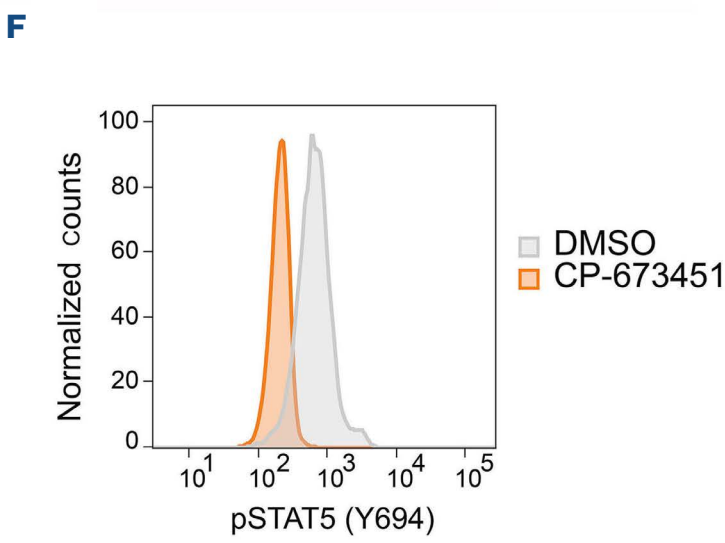

Continued on following page.

Figure 1. A novel *MYH9::PDGFRB* fusion gene identified in a T-cell lymphoblastic lymphoma patient can transform Ba/F3 cells to cytokine-independent growth. (A) Schematic representation of the novel *MYH9::PDGFRB* fusion gene identified in a case of pediatric T-cell lymphoblastic lymphoma (T-LBL). The fusion gene consists of exon 1-25 from *MYH9* (chromosome 22) linked to exon 10-23 from *PDGFRB* (chromosome 5). The fusion retains the motor domain and part of the myosin tail from MYH9 and the protein tyrosine kinase domain of PDGFRB. Figure was made using ProteinPaint (SJ-15-0021, St. Jude). (B) Immunohistochemistry for PDGFRB was performed on lymph nodes from the same T-LBL case with the *MYH9::PDGFRB* fusion gene. Expression of PDGFRB in both diagnostic and relapse sample is compared to healthy tissue (lymph node and thymus). (C) Proliferation of Ba/F3 cells with or without MYH9::PDGFRB expression following 7 days after IL-3 withdrawal. Proliferation was measured using cell counts. Data show mean ± SEM (Standard Error of Mean) (N=3). (D) Cell viability of Ba/F3 cells expressing MYH9::PDGFRB and JAK3(M511I) treated for 72 hours with the PDGFRB inhibitor CP-673451 (MYH9::PDGFRB IC_{50}=9.448 nM). Cell viability was measured using cells counts. Data show mean±SEM (N=3). (E) Phosphorylation of PDGFRB (pPDGFRB) at Y751 analyzed using western blotting. MYH9::PDGFRB expressing Ba/F3 cells were treated with 0 or 1 μM CP-673451 for one hour. (F) STAT5 phosphorylation (pSTAT5 (Y694)) flow cytometry analysis of MYH9::PDGFRB expressing Ba/F3 cells treated with DMSO vehicle control or 1 μM CP-673451 for one hour.

monitored over time for the development of leukemia. A fraction of the transduced HSPC were also kept in culture *ex vivo*, in the absence of cytokines. The GFP^+ MYH9::PDGFRB transduced HSPC had a survival advantage compared to non-transduced GFP^- cells *ex vivo* (*Online Supplementary Figure S3A*). *In vivo*, the recipient mice initially had an expansion of GFP^+ cells characterized by a moderate increase in WBC (*Online Supplementary Figure S3B*). Five out of 6 MYH9::PDGFRB mice developed either a myeloid (N=3) or T-cell (N=2) proliferative malignancy (Figure 2B, *Online Supplementary Table S1*), characterized by enlarged spleens and/or thymi (Figure 2C). Immunophenotyping via flow cytometry was performed on infiltrated organs (BM, spleen, thymus), with mice displaying enlarged spleens without thymoma characterized by a major $Gr1^+CD11b^+$ myeloid clone, while mice with enlarged spleen and thymoma showed a major single positive CD8 and double positive CD4/CD8 lymphoid clone (Figure 2D; gating strategy illustrated in *Online Supplementary Figure S3C*).

This is in contrast to the EBF1::PDGFRB mice, of which none of the mice developed leukemia (Figure 2B, *Online Supplementary Table S2*). Cause of death of these EBF1::PDGFRB mice was unclear. While some of these mice rapidly lost body weight and reached predetermined experimental endpoints, we observed no signs of leukemia or overt pathology at secondary sites, including spleen, liver, or lymph nodes.

Increased PDGFRB expression in T-cell acute lymphoblastic leukemia compared to normal T cells and thymocytes

We next hypothesized that ectopic activation of PDGFRB might occur more generally within T-ALL/T-LBL cases, potentially even in the absence of chromosomal translocations. We first investigated mRNA expression levels of PDGFRB in normal T cells. *PDGFRB* is expressed at early immature stages in normal T-cell development and decreases after β-selection (Figure 3A). In contrast, analysis of T-ALL patient samples showed robust PDGFRB expression across all subtypes, with significantly higher levels in the TLX3 and HOXA subgroups (Figure 3B). We also screened a panel of T-ALL cell lines for PDGFRB protein levels using western blot analysis. PDGFRB protein levels correlated nicely with *PDGFRB* RNA levels. High PDGFRB levels were observed in the T-ALL cell lines CTV-1 and DND-41 alongside the SEM BCP-ALL cell line (Figure 3C). However, only CTV-1 and SEM showed phosphorylation and activation of the receptor (Figure 3C). We then extended our analysis to a panel of available T-ALL/T-LBL PDX samples and identified 5 out of 12 with high PDGFRB protein levels: 4 T-ALL PDX and 1 T-LBL. All but one also showed phosphorylation of the receptor (Figure 3D). Whole exome sequencing of PDX samples did not reveal any *PDGFRB* point mutation that could explain the phosphorylation status of the receptor.

PDGFRB receptor phosphorylation status determines sensitivity to the inhibitor CP-673451

We next determined whether $PDGFRB^+$ T-ALL cell lines DND-41 and CTV-1 were sensitive to the selective PDGFRB inhibitor CP-673451. Only CTV-1 was sensitive (IC_{50} = 230 nM) whilst DND-41 was resistant (IC_{50} >500 nM), similar to T-ALL cell lines without PDGFRB expression (Figure 4A). Due to limited *ex vivo* proliferating capacity of some of the PDX samples, we could only use 6 T-ALL/T-LBL PDX for *ex vivo* drug sensitivity determination. Unfortunately, only one of these *ex vivo* cultured PDX showed expression and activation of the PDGFRB receptor, T-ALL1 PDX. As was observed for CTV-1, only the T-ALL1 PDX sample with PDGFRB activation was highly sensitive to CP-673451 (T-ALL1 IC_{50} <5 nM) (Figure 4B). For the other T-ALL PDX with activated PDGFRB that could not be assayed in *ex vivo* proliferation experiments, downregulation of pPDGFRB after acute PDGFRB inhibition (1 hour, 1 μM CP-673451) was confirmed by western blotting (*Online Supplementary Figure S4A*). Inhibition of PDGFRB was also associated with loss of downstream signaling, indicated by loss of phosphorylation of PDGFRB (Tyr751), pSTAT3 (Tyr705), pSTAT5 (Tyr694), pGSK3β (Ser9), and pAKT (Ser473) (Figure 4C, *Online Supplementary Figure S4B*).

The CTV-1 cell line is resistant to dexamethasone, a key component of induction therapy for T-ALL/T-LBL.[7,27-29] The T-LBL patient with *MYH9::PDGFRB* fusion identified in this

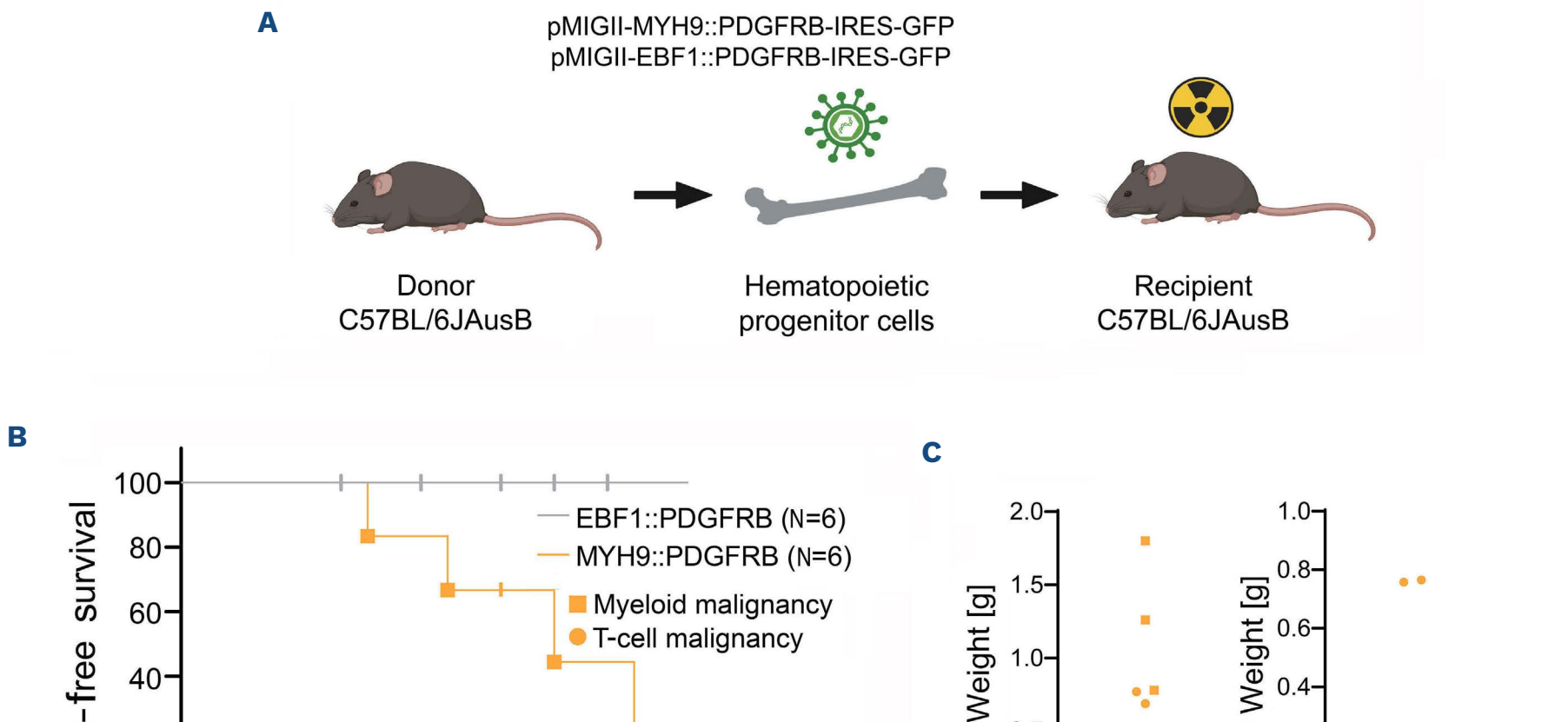

Figure 2. *MYH9::PDGFRB* drives acute leukemia in a murine bone marrow transplant model. (A) Schematic overview of syngeneic bone marrow transplant model. Created with BioRender.com (B) Kaplan-Meier event-free survival curve of *MYH9::PDGFRB* (N=6) /*EBF1::PDGFRB* mice (N=6). (C) Weight of spleen and thymus from MYH9::PDGFRB mice that reached event. (D) Immunophenotyping by flow cytometry of GFP⁺ cells from infiltrated organs. Representative figures for myeloid clone (spleen from mouse 4) and lymphoid thymoma (thymus from mouse 1).

study also showed a poor corticosteroid response. Therefore, we next tested whether CP-673451 could act synergistically with dexamethasone. Treatment of CP-673451 in combination with dexamethasone in CTV-1 resulted in strong synergism (Mean Bliss score = 14.66) (Figure 4D). Taken together, these results show that inhibition of active PDGFRB, alone or in combination with glucocorticoids, results in reduced cell viability in a T-ALL cell line.

Selective inhibition of *PDGFRB in vivo* results in significant leukemia growth delay

Finally, we evaluated the *in vivo* potential of PDGFRB inhibition using CP-673451 as a new therapeutic strategy in T-ALL/T-LBL. NSG-SGM3 mice were injected intravenously with T-ALL1 PDX samples with hyperactive PDGFRB signaling. After leukemia initiation, mice were randomized in two groups and treated for two weeks (5 days on / 2 days off)

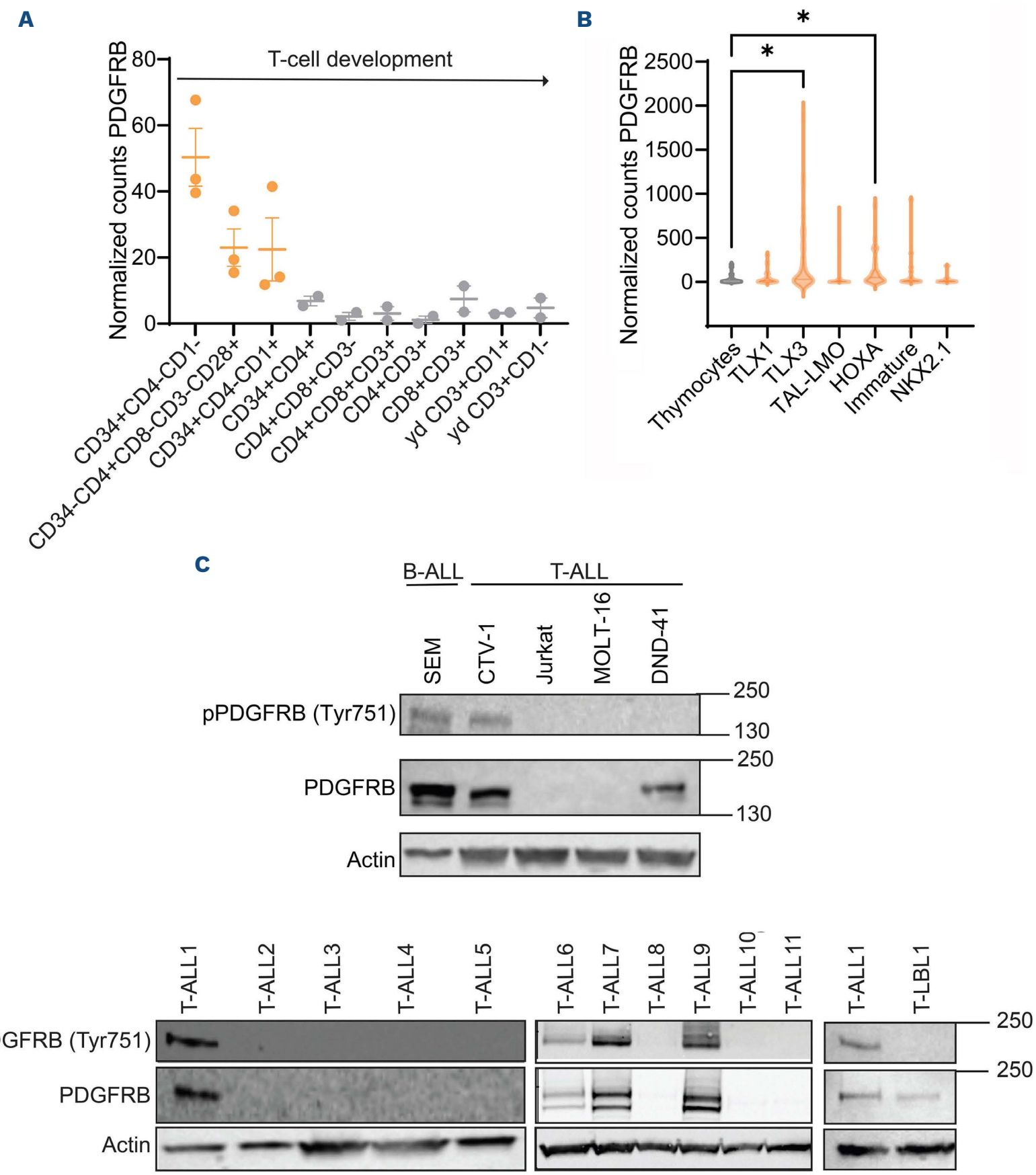

Figure 3. Increased PDGFRB expression in T-cell acute lymphoblastic leukemia compared to normal T cells and thymocytes. (A) Normalized counts of PDGFRB RNA expression in normal T-cell subsets (23 samples). (B) Normalized counts of PDGFRB RNA expression in normal thymocytes *versus* T-cell acute lymphoblastic leukemia (T-ALL) subgroups (292 samples). (C) (p)PDGFRB (Tyr751) western blot analysis of a panel of T-ALL and B-cell acute lymphoblastic leukemia (B-ALL) cell lines. (D) (p)PDGFRB (Tyr751) western blot analysis of a panel of T-ALL/T-cell lymphoblastic lymphoma (T-LBL) patient-derived xenograft samples. *P<0.05.

with CP-673451 (20 mg/kg) or vehicle alone (90% PEG300, 10% N-methylpyrrolidone). Mice were sacrificed at the end of the 2-week treatment. PDGFRB inhibition caused a significant delay in leukemia progression and leukemic burden as evaluated by the percentage of hCD45⁺ cells in PB (Figure 5A) (P<0.01) and BM (Figure 5B) (P<0.0001), as by spleen weight (Figure 5C) (P<0.0001). The treatment was well tolerated, with no significant differences in loss in body weight between vehicle and treatment group (*Online Supplementary Figure S5*). These results compellingly show the therapeutic potential of PDGFRB inhibition in T-ALL/T-LBL patients with PDGFRB hyperactivation.

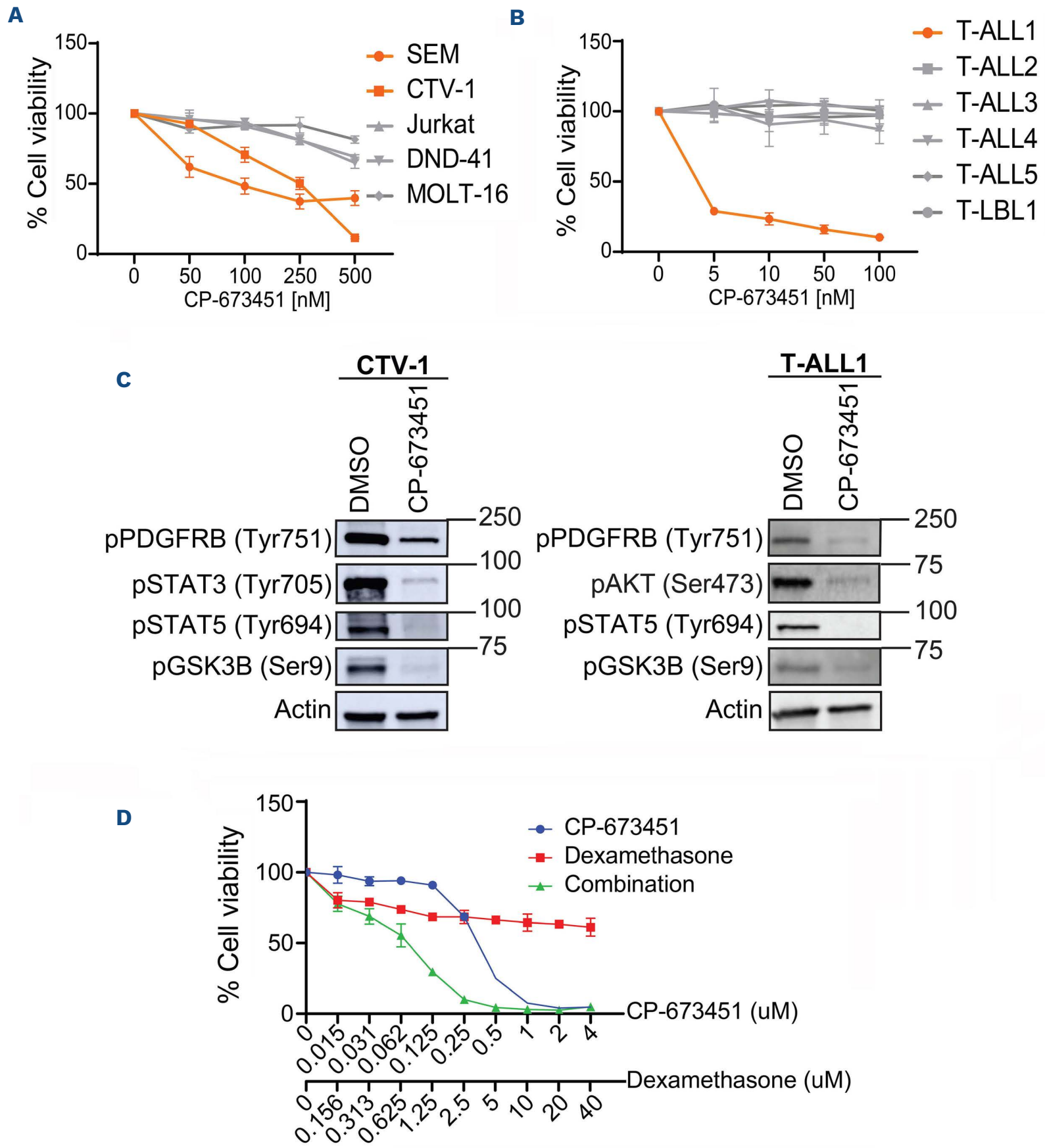

Figure 4. PDGFRB receptor phosphorylation status determines sensitivity to the inhibitor CP-673451. (A) Cell viability assay of a panel of T-cell acute lymphoblastic leukemia (T-ALL) and B-cell acute lymphoblastic leukemia (B-ALL) cell lines treated with CP-673451 (0, 50, 100, 250, 500 nM) for 72 hours. Data show mean±Standard Error of Mean (SEM) (N=3). (B) Cell viability assay of a panel of T-ALL/T-cell lymphoblastic lymphoma (T-LBL) patient-derived xenograft (PDX) samples treated with CP-673451 (0, 5, 10, 50, 100 nM) for 72 hours. Data show mean±SEM (N=3). (C) Western blot analysis on CTV-1 and T-ALL1 treated with 0, 10 (TALL-1) or 500 nM (CTV-1) CP-673451 for 72 hours. (D) Cell viability assay on CTV-1 treated with CP-673451 (0 - 0.015 - 0.031 - 0.062 - 0.125 - 0.25 - 0.5 - 1 - 2 - 4 μM) and/or dexamethasone (0 - 0.156 - 0.312 - 0.625 - 1.25 - 2.5 - 5 - 10 - 20 - 40 μM) for 72 hours. Data show mean±SEM (N=3).

Discussion

Identifying genetic drivers of T-ALL remains a priority for the development of novel targeted therapeutic strategies, especially for those patients with relapsed or refractory disease. In this study, we identified a novel *MYH9::PDGFRB* fusion gene in a relapsed chemo-resistant T-LBL patient. *MYH9* is an evolutionary conserved gene located on chromosome 22 and encodes for the myosin-9 protein, which forms the heavy chain of the cytoplasmic non-muscle myosin IIA3 (NMM IIA).[30] MYH9 is an actin binding molecular motor and is involved in cell adhesion, migration, as well as signal transduction.[31] It is the only myosin class II protein that is highly expressed in T cells and has been linked to T-cell motility,[32] as well as immunological synapses and T-cell activation.[33] Fusions involving *MYH9* have been found in other disorders and include *MYH9::FLT3*,[34] *MYH9::ROS1*,[35] and *MYH9::USP6*.[36] Similarly, PDGFRB fusion proteins have been described in myeloid disorders and myeloid leukemia[15,20,37,38] and, indeed, aberrant expression of this receptor tyrosine kinase has been described in several cancer entities.[39,40]

In our study, we demonstrate that this new MYH9::PDGFRB fusion has oncogenic capacity both *in vitro* to drive cytokine-independent growth and *in vivo* to drive leukemia using a BMT model. Mechanistically, PDGFRB fusions require oligomerization domains present in the fusion partners for their constitutive activation.[26] In the *MYH9::PDGFRB* fusion described here, exons 1-25 of MYH9 are retained, which includes the coiled coil regions on the myosin tail that are speculated to promote dimerization within the cytoplasm rather than at the plasma membrane.[30] However, our *in vivo* BM transplant model also supports a model where the fusion partner of PDGFRB provides an important cellular context in addition to oligomerization, with marked differences in leukemogenic potential between EBF1::PDGFRB and MYH9::PDGFRB fusions, with only the latter resulting in mice developing a mixed phenotype proliferative disorder/leukemia. Of note, an alternative activation mechanism for a PDGFRB fusion was also recently demonstrated with an out of frame CD74::PDGFRB fusion resulting in the expression of a 'loose' kinase that equally caused leukemic transformation.[38]

Besides the reported rare *PDGFRB* translocations and fusion products, recurrent activating point mutations in *PDGFRB* have not been described in T-ALL/T-LBL patients. Nevertheless, we observed that 4 out of the 12 (33%) analyzed PDX samples have hyperactive PDGFRB signaling. More research will be necessary to resolve how the pathway is activated in these patients. Based on our RNA expression data (*data not shown*), we did not observe autocrine expression of PDGF ligands in T-ALL cell lines, T-ALL patients, or PDX samples. Also, the *ex vivo* effects of PDGFRB inhibition were observed in the absence of paracrine stimulation. Of note, we have generated transgenic mice with conditional overexpression of the wild-type PDGFRB receptor. Although gain of *Pdgfrb* expression was confirmed at the RNA and protein level, this was not sufficient to hyperactivate the pathway (*Online Supplementary Figure S6*). When intercrossed with *Pten* conditional knockout mice, a spontaneous T-ALL mouse model, also no effects of wild-type PDGFRB overexpression were seen on T-ALL latency. Our combined results indicate that hyperactivation of the PDGFRB pathway in T-ALL is cell-intrinsic and independent of the presence of ligands. Possible mechanisms of activation include cross-talk between other signaling pathways such as NRP1,[41] downregulation of PDGFRB inhibitors,[42] and upregulation of the dephosphorylator SHP-2.[43]

We show that the PDGFRB is active via phosphorylation

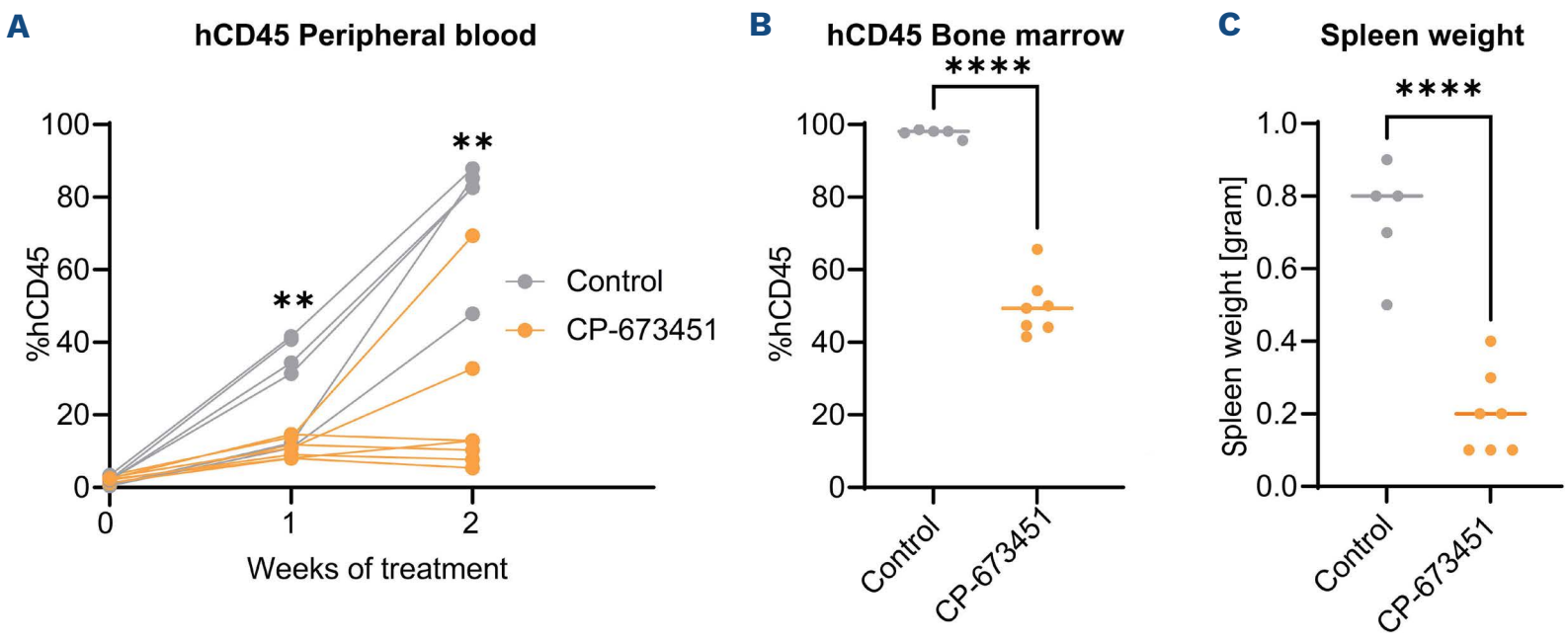

Figure 5. Selective inhibition of PDGFRB *in vivo* results in significant leukemia growth delay. (A) % hCD45$^+$ cells in peripheral blood at start of treatment (week 0), 1 and 2 weeks after start of treatment analyzed using flow cytometry. (B) % hCD45$^+$ cells in bone marrow at end of treatment (2 weeks) analyzed using flow cytometry. (C) Spleen weight at end of treatment (2 weeks). **P<0.01, ****P<0.0001.

at residue 751 in 4 T-ALL PDX samples and is decreased upon treatment with the PDGFRB inhibitor CP-673451. Evaluation of the pPDGFRB levels on primary patient material may be an efficient biomarker to predict sensitivity towards CP-673451. In the clinic, patients with *PDGFRB* rearrangements have been found to be refractory to conventional chemotherapy providing support for using PDGFRB inhibitors in the clinic.[17-19] In general, the multikinase inhibitors sunitinib and dasatinib have been used to block PDGFRB, but these also block SRC family kinases (SRC, LCK, YES, FYN), c-KIT and EPHA2, and can, therefore, cause unwanted side effects such as cardiac toxicity.[44,45] CP-673451 is a selective PDGFRB inhibitor with a 10-fold higher selectivity for PDGFRB than PDGFRA. It is also >200-fold more selective for PDGFRB compared to other tyrosine kinase receptors including C-KIT, VEGFR2, EGFR and SRC. The adenine group of CP-673451 binds the ATP binding pocket of PDGFRB and prevents enzymatic activation upon ligand binding.[46] This inhibitor has already been shown to be effective in several types of cancers, including lung cancer,[47,48] sarcoma,[39] and glioblastoma.[49] Here we showed that CP-673451 was able to slow leukemic growth *in vitro* but only on cells that had active pPDGFRB present. We provide evidence that CP-673451 was able to slow leukemia growth of a PDX *in vivo* as a single agent. However, the small molecule CP-673451 is still considered a tool compound and requires improved pharmacokinetics prior to its potential use for PDGFRB inhibition in T-ALL/T-LBL patients. Other less selective but clinically approved PDGFRB inhibitors, such as imatinib, could be used to rapidly translate our research results into clinical applications.

Although we do see a significant therapeutic effect of PDGFRB inhibition on the *in vivo* leukemic burden, 2 out of the 6 CP-673451 treated PDX animals showed increased leukemia progression at the end of the two weeks of treatment. Potentially, these leukemic animals rapidly acquire resistance to the monotherapy, and this would suggest that PDGFRB inhibition would best be combined with other T-ALL therapeutics, e.g., glucocorticoids or L-asparaginase. Indeed, glucocorticoid resistance remains a major problem in T-ALL/T-LBL patients, and we showed here that CP-673451 was also able to restore glucocorticoid sensitivity.

Using phosphoproteomics to identify activated signaling pathways in T-ALL has recently been suggested as a profiling strategy to identify targeted kinase inhibitor therapies.[50] Our data indicate that phosphorylation of PDGFRB may be a feature of a subgroup of T-ALL, potentially in the absence of activating fusions. This lends further support to the idea that phosphoproteomic analysis of patient samples could identify targetable kinases and combination treatment strategies,[51] particularly as preclinical testing of new, specific, small molecule inhibitors have promising activity in T-ALL samples.[52] Our study shows that PDGFRB activation can be therapeutically targeted by the PDGFRB inhibitor CP-673451 in T-ALL/T-LBL. In addition, our work suggests that phosphorylated PDGFRB could serve as a valuable biomarker to identify patients that could benefit from PDGFRB inhibition.

Disclosures

No conflicts of interest to disclose.

Contributions

SDC, RDS, CEdB, SG and PVV are responsible for study concept. BP is responsible for methodology. SDC is responsible for formal analysis. SDC, RDS, BL, LR, HJK, AR, JR and MvdL are responsible for the investigation. LB, NVR, JV, RBL, PN, FvD, MM, TP, TL and BDM are responsible for resources. SDC is responsible for data curation. SDC, TL, CEdB and SG wrote the original draft. SDC, RDS, BL, LR, HJK, AR, LB, NVR, BP, MVdL, JV, RBL, PN, FvD, MM, TL, BDM, CEdB and SG wrote, reviewed and edited the manuscript. SDC and BP are responsible for visualization. CEdB, SG and PVV supervised the study. SDC, SG and PVV are responsible for project administration. SG and PVV are responsible for funding acquisition. All authors have read and agreed to the published version of the manuscript.

Acknowledgments

We would like to thank Professor Richard B. Lock for providing T-ALL PDX samples. We also thank Prof. Paul Ekert and Prof. Kris Gevaert for constructive discussions and proofreading the manuscript.

Funding

The Van Vlierberghe, Goossens and Ntziachristos laboratories are supported by the Research Foundation Flanders (FWO-G0F4721N, SBO-S002322N), Ghent University, a Flanders interuniversity consortium grant (BOF23/IBF/042) and Cancer Research Institute Ghent (CRIG) partnership grant. The computational resources and services used in this work were provided by the VSC (Flemish Supercomputers Center), funded by the Research Foundation-Flanders (FWO). MRM is funded by the Great Ormond Street Childrens Charity. The de Bock laboratory is supported by the Children's Cancer Institute Team Leader funds, UNSW RIS grant RG213825-C, NHMRC Ideas grant APP1181666. This work was supported in part by vzw Kinderkankerfonds (grant to TL).

Data-sharing statement

Data related to the study are available on request.

References

1. Lepretre S, Graux C, Touzart A, Macintyre E, Boissel N. Adult T-type lymphoblastic lymphoma: treatment advances and prognostic indicators. Exp Hematol. 2017;51:7-16.
2. Burkhardt B, Mueller S, Khanam T, Perkins SL. Current status and future directions of T-lymphoblastic lymphoma in children and adolescents. Br J Haematol. 2016;173(4):545-559.
3. Iacobucci I, Mullighan CG. Genetic basis of acute lymphoblastic leukemia. J Clin Oncol. 2017;35(9):975-983.
4. JE YL, Shao Y, Maciaszek J, et al. The genomic landscape of pediatric and young adult T-lineage acute lymphoblastic leukemia. Nat Genet. 2017;49(8):1211-1220.
5. Jabbour E, O'Brien S, Konopleva M, Kantarjian HM. New insights into the pathophysiology and therapy of adult acute lymphoblastic leukemia. Cancer. 2015;121(15):2517-2528.
6. Hofmans M, Suciu S, Ferster A, et al. Results of successive EORTC-CLG 58 881 and 58 951 trials in paediatric T-cell acute lymphoblastic leukaemia (ALL). Br J Haematol. 2019;186(5):741-753.
7. Bassan R, Bourquin JP, DeAngelo DJ, Chiaretti S. New approaches to the management of adult acute lymphoblastic leukemia. J Clin Oncol. 2018;36(35):3504-3519.
8. Cordo V, van der Zwet JCG, Canté-Barrett K, Pieters R, Meijerink JPP. T-cell acute lymphoblastic leukemia: a roadmap to targeted therapies. Blood Cancer Discov. 2021;2(1):19-31.
9. Girardi T, Vicente C, Cools J, De Keersmaecker K. The genetics and molecular biology of T-ALL. Blood Cancer Discov. 2017;129(9):1113-1123.
10. Maude SL, Dolai S, Delgado-Martin C, et al. Efficacy of JAK/STAT pathway inhibition in murine xenograft models of early T-cell precursor (ETP) acute lymphoblastic leukemia. Blood Cancer Discov. 2015;125(11):1759-1767.
11. Graux C, Cools J, Melotte C, et al. Fusion of NUP214 to ABL1 on amplified episomes in T-cell acute lymphoblastic leukemia. Nat Genet. 2004;36(10):1084-1089.
12. Quintás-Cardama A, Tong W, Manshouri T, et al. Activity of tyrosine kinase inhibitors against human NUP214-ABL1-positive T cell malignancies. Leukemia. 2008;22(6):1117-1124.
13. Deenik W, Beverloo HB, van der Poel-va Luytgaarde SCPAM, et al. Rapid complete cytogenetic remission after upfront dasatinib monotherapy in a patient with a NUP214-ABL1-positive T-cell acute lymphoblastic leukemia. Leukemia. 2009;23(3):627-629.
14. Shi Y, Beckett MC, Blair HJ, et al. Phase II-like murine trial identifies synergy between dexamethasone and dasatinib in T-cell acute lymphoblastic leukemia. Haematologica. 2021;106(4):1056-1066.
15. Demoulin JB, Montano-Almendras CP. Platelet-derived growth factors and their receptors in normal and malignant hematopoiesis. Am J Blood Res. 2012;2(1):44-56.
16. Rogers MA, Fantauzzo KA. The emerging complexity of PDGFRs: activation, internalization and signal attenuation. Biochem Soc Trans. 2020;48(3):1167-1176.
17. Shah KP, Carrol CM, Mosse C, Yenamandra A, Borinstein SC. Sustained remission in a patient with PDGFR-beta-rearranged T-lymphoblastic lymphoma and complete remission with dasatinib. Pediatr Blood Cancer. 2020;67(1):e28026.
18. Heilmann AM, Schrock AB, He J, et al. Novel PDGFRB fusions in childhood B- and T-acute lymphoblastic leukemia. Leukemia. 2017;31(9):1989-1992.
19. Zabriskie MS, Antelope O, Verma AR, et al. A novel AGGF1-PDGFRb fusion in pediatric T-cell acute lymphoblastic leukemia. Haematologica. 2018;103(2):87-91.
20. Di Giacomo D, Quintini M, Pierini V, et al. Genomic and clinical findings in myeloid neoplasms with PDGFRB rearrangement. Ann Hematol. 2022;101(2):297-307.
21. de Vree PJP, de Wit E, Yilmaz M, et al. Targeted sequencing by proximity ligation for comprehensive variant detection and local haplotyping. Nat Biotechnol. 2014;32(10):1019-1025.
22. Van Thillo Q, De Bie J, Seneviratne JA, et al. Oncogenic cooperation between TCF7-SPI1 and NRAS(G12D) requires β-catenin activity to drive T-cell acute lymphoblastic leukemia. Nat Commun. 2021;12(1):4164.
23. Lock RB, Liem N, Farnsworth ML, et al. The nonobese diabetic/severe combined immunodeficient (NOD/SCID) mouse model of childhood acute lymphoblastic leukemia reveals intrinsic differences in biologic characteristics at diagnosis and relapse. Blood. 2002;99(11):4100-4108.
24. Townsend EC, Murakami MA, Christodoulou A, et al. The public repository of xenografts enables discovery and randomized phase II-like trials in mice. Cancer Cell. 2016;29(4):574-586.
25. Fernandez-Prado R, Carriazo-Julio SM, Torra R, Ortiz A, Perez-Gomez MV. MYH9-related disease: it does exist, may be more frequent than you think and requires specific therapy. Clin Kidney J. 2019;12(4):488-493.
26. Welsh SJ, Churchman ML, Togni M, Mullighan CG, Hagman J. Deregulation of kinase signaling and lymphoid development in EBF1-PDGFRB ALL leukemogenesis. Leukemia. 2017;32(1):38-48.
27. De Smedt R, Morscio J, Goossens S, Van Vlierberghe P. Targeting steroid resistance in T-cell acute lymphoblastic leukemia. Blood Rev. 2019;38:100591.
28. Inaba H, Mullighan CG. Pediatric acute lymphoblastic leukemia. Haematologica. 2020;105(11):2524-2539.
29. Marks DI, Rowntree C. Management of adults with T-cell lymphoblastic leukemia. Blood. 2017;129(9):1134-1142.
30. Pecci A, Ma X, Savoia A, Adelstein RS. MYH9: structure, functions and role of non-muscle myosin IIA in human disease. Gene. 2018;664:152-167.
31. Asensio-Juárez G, Llorente-Gonzalez C, Vicente-Manzanares M. Linking the landscape of MYH9-related diseases to the molecular mechanisms that control non-muscle myosin II-A function in cells. Cells. 2020;9(6):1458.
32. Jacobelli J, Chmura SA, Buxton DB, Davis MM, Krummel MF. A single class II myosin modulates T cell motility and stopping, but not synapse formation. Nat Immunol. 2004;5(5):531-538.
33. Kumari S, Vardhana S, Cammer M, et al. T lymphocyte myosin IIA is required for maturation of the immunological synapse. Front Immunol. 2012;3:230.
34. Clark EE, Walton M, Chow LML, Boyd JT, Yohannan MD, Arya S. Disseminated juvenile xanthogranuloma with a novel MYH9-FLT3 fusion presenting as a blueberry muffin rash in a neonate. AJP Rep. 2023;13(1):e5-e10.
35. Tsuda T, Takata N, Hirai T, Masaki Y, Ishizawa S, Taniguchi H. Rare MYH9-ROS1 fusion gene-positive lung adenocarcinoma showing response to entrectinib treatment: a case study. Case Rep Oncol. 2022;15(1):376-381.
36. Pižem J, Matjašic A, Zupan A, Luzar B, Šekoranja D, Dimnik K. Fibroma of tendon sheath is defined by a USP6 gene fusion-morphologic and molecular reappraisal of the entity. Mod Pathol. 2021;34(10):1876-1888.
37. Andrae J, Gallini R, Betsholtz C. Role of platelet-derived growth

factors in physiology and medicine. Genes Dev. 2008;22(10):1276-1312.
38. Sadras T, Jalud FB, Kosasih HJ, et al. Unusual PDGFRB fusion reveals novel mechanism of kinase activation in Ph-like B-ALL. Leukemia. 2023;37(4):905-909.
39. Ehnman M, Missiaglia E, Folestad E, et al. Distinct effects of ligand-induced PDGFRα and PDGFRβ signaling in the human rhabdomyosarcoma tumor cell and stroma cell compartments. Cancer Res. 2013;73(7):2139-2149.
40. Mazzu YZ, Hu Y, Shen Y, Tuschl T, Singer S. miR-193b regulates tumorigenesis in liposarcoma cells via PDGFR, TGFβ, and Wnt signaling. Sci Rep. 2019;9(1):3197.
41. Rizzolio S, Tamagnone L. Neuropilins as signaling hubs, controlling tyrosine kinases and other cell surface receptors. In: The neuropilins: role and function in health and disease; 2017: p. 23-39. https://doi.org/10.1007/978-3-319-48824-0_3 Accessed August 2023.
42. Chen D, Li Y, Mei Y, et al. miR-34a regulates mesangial cell proliferation via the PDGFR-β/Ras-MAPK signaling pathway. Cell Mol Life Sci. 2014;71(20):4027-4042.
43. Pandey P, Khan F, Upadhyay TK, Seungjoon M, Nyeo Park M, Kim B. New insights about the PDGF/PDGFR signaling pathway as a promising target to develop cancer therapeutic strategies. Biomed Pharmacother. 2023;161:114491.
44. Liu Y, Li Y, Wang Y, et al. Recent progress on vascular endothelial growth factor receptor inhibitors with dual targeting capabilities for tumor therapy. J Hematol Oncol. 2022;15(1):89.
45. Chintalgattu V, Rees ML, Culver JC, et al. Coronary microvascular pericytes are the cellular target of sunitinib malate induced cardiotoxicity. Sci Transl Med. 2013;5(187):187ra69.
46. Roberts WG, Whalen PM, Soderstrom E, et al. Antiangiogenic and antitumor activity of a selective PDGFR tyrosine kinase inhibitor, CP-673,451. Cancer Res. 2005;65(3):957-966.
47. Yin L, He J, Xue J, et al. PDGFR-β inhibitor slows tumor growth but increases metastasis in combined radiotherapy and Endostar therapy. Biomed Pharmacother. 2018;99:615-621.
48. Xi Y, Chen M, Liu X, Lu Z, Ding Y, Li D. CP-673451, a platelet-derived growth-factor receptor inhibitor, suppresses lung cancer cell proliferation and migration. Onco Targets Ther. 2014;7:1215-1221.
49. Lane R, Cilibrasi C, Chen J, et al. PDGF-R inhibition induces glioblastoma cell differentiation via DUSP1/p38MAPK signalling. Oncogene. 2022;41(19):2749-2763.
50. Cordo V, Meijer MT, Hagelaar R, et al. Phosphoproteomic profiling of T cell acute lymphoblastic leukemia reveals targetable kinases and combination treatment strategies. Nat Commun. 2022;13(1):1048.
51. van der Zwet JCG, Cordo V, Canté-Barrett K, Meijerink JPP. Multi-omic approaches to improve outcome for T-cell acute lymphoblastic leukemia patients. Adv Biol Regul. 2019;74:100647.
52. Yoshimura S, Panetta JC, Hu J, et al. Preclinical pharmacokinetic and pharmacodynamic evaluation of dasatinib and ponatinib for the treatment of T-cell acute lymphoblastic leukemia. Leukemia. 2023;37(6):1194-1203.